Emulation of the laparoscopic environment for image-guided liver surgery via an abdominal phantom system with anatomical ligamenture

Jon S. Heiselman[1,2], Jarrod A. Collins[1,2], Logan W. Clements[1,2], Jared A. Weis[1], Amber L. Simpson[3], Sunil K. Geevarghese[4], William R. Jarnagin[3], and Michael I. Miga[1,2,5,6]

[1]Department of Biomedical Engineering, Vanderbilt University, Nashville, TN
[2]Vanderbilt Institute in Surgery and Engineering, Vanderbilt University, Nashville, TN
[3]Hepatopancreatobiliary Service, Department of Surgery, Memorial Sloan-Kettering Cancer Center, New York, NY
[4]Division of Hepatobiliary Surgery and Liver Transplantation, Vanderbilt University Medical Center, Nashville, TN
[5]Department of Radiology and Radiological Sciences, Vanderbilt University Medical Center, Nashville, TN
[6]Department of Neurological Surgery, Vanderbilt University Medical Center, Nashville, TN

ABSTRACT

In order to rigorously validate techniques for image-guided liver surgery (IGLS), an accurate mock representation of the intraoperative surgical scene with quantifiable localization of subsurface targets would be highly desirable. However, many attempts to reproduce the laparoscopic environment have encountered limited success due to neglect of several crucial design aspects. The laparoscopic setting is complicated by factors such as gas insufflation of the abdomen, changes in patient orientation, incomplete organ mobilization from ligaments, and limited access to organ surface data. The ability to accurately represent the influences of anatomical changes and procedural limitations is critical for appropriate evaluation of IGLS methodologies such as registration and deformation correction. However, these influences have not yet been comprehensively integrated into a platform usable for assessment of methods in laparoscopic IGLS. In this work, a mock laparoscopic liver simulator was created with realistic ligamenture to emulate the complexities of this constrained surgical environment for the realization of laparoscopic IGLS. The mock surgical system reproduces an insufflated abdominal cavity with dissectible ligaments, variable levels of incline matching intraoperative patient positioning, and port locations in accordance with surgical protocol. True positions of targets embedded in a tissue-mimicking phantom are measured from CT images. Using this setup, image-to-physical registration accuracy was evaluated for simulations of laparoscopic right and left lobe mobilization to assess rigid registration performance under more realistic laparoscopic conditions. Preliminary results suggest that non-rigid organ deformations and the region of organ surface data collected affect the ability to attain highly accurate registrations in laparoscopic applications.

Keywords: laparoscopy, image guidance, conoprobe, liver phantom, hepatic ligaments, surgical simulator

1. INTRODUCTION

Soft tissue deformation and inconsistent data quality can considerably contribute to registration error in image-guided liver surgery (IGLS). These factors necessitate that registration methods be quantitatively validated under realistic conditions. However, intraoperative clinical validation through intraoperative CT, intraoperative MR, or intraoperative ultrasound can be prohibitively burdensome, expensive, or challenging. Although validation strategies using intraoperative imaging have been explored by groups including Heizmann et al.[1] and Clements et al.[2], other *in vivo* validation approaches mostly rely on surface residual error[3,4] or manual selection of surface-based landmarks[5]. However, surface accuracy may not be indicative of subsurface registration accuracy. Due to these limitations, efforts to quantify IGLS registration accuracy often employ well-documented tissue-mimicking liver phantoms to supplement the more restricted capabilities of *in vivo* validation[4,5]. While somewhat intuitive, challenges remain; namely, in order to appropriately validate registration and navigation techniques in a phantom environment, an accurate representation of the intraoperative surgical scene must be established. The phantom setup used by Rucker et al.[4] incorporated surgical packing material to simulate intraoperative deformation caused by placement of laparotomy pads beneath the liver during open procedures. Banovac et al.[6] developed a liver phantom that reproduced respiratory motion for validation of liver biopsy guidance. Replicating the relevant dynamics of the surgical environment is an important concern towards providing value to the phantom system. However, the ability to simulate the intricacies of the laparoscopic environment has not been adequately developed. In previous work, a silicone liver phantom was placed in a laparoscopic trainer box in an attempt to evaluate a deformation correction strategy in the laparoscopic setting[7]. However, this study failed to account for the fundamental anatomical changes that distinguish laparoscopic from open procedures.

In laparoscopic liver resection, deformation between the preoperative and intraoperative positions of the organ primarily arises from three sources. First, the abdominal cavity is insufflated with carbon dioxide during the procedure. This process displaces the abdominal wall, the diaphragm, and the tissues surrounding the liver. With the falciform ligament attaching the anterior side of the liver to the ventral wall and the left and right triangular ligaments attaching the superior side of the liver to the diaphragm (Figure 1, left), insufflation can cause significant motion of the organ. Zijlmans et al.[8] found that abdominal insufflation caused the liver to shift up 35mm in a porcine study. In humans, we have observed that insufflation during laparoscopy causes suspension of the liver from the anterosuperior ligaments, including the falciform and triangular ligaments (Figure 1, center). In this work, we propose that suspension of the liver from these ligament attachments plays a central role in liver deformation during laparoscopic procedures.

In addition to insufflation, a second source of deformation arises from changes in patient positioning between preoperative imaging and the intraoperative presentation. While preoperative images are acquired with the patient completely supine, intraoperative forward inclines of 10–30° in the reverse Trendelenburg position are common. The forward incline changes the orientation of the liver with respect to gravity and contributes to deformation between intraoperative and preoperative states. More specifically, the forward incline may cause a partial shift in mechanical support from the falciform ligament, located anterior to the liver, onto the left and right triangular ligaments, located superior to the liver.

Finally, substantial soft tissue deformation can result from organ mobilization, where the supporting ligaments are dissected to improve the manipulability of the organ. In laparoscopic liver resections, the liver is usually incompletely mobilized from its ligamenture. In left lobe mobilization, the falciform and left triangular ligaments are typically divided whereas in right lobe mobilization, the falciform and right triangular ligaments are divided instead. As shown in Figure 1 (right), the dissection of these ligaments can produce considerable deformation as the structures suspending the organ are cut away. In a phantom system, these conformational changes cannot be reproduced easily without placing the phantom under explicit control by the supporting ligaments.

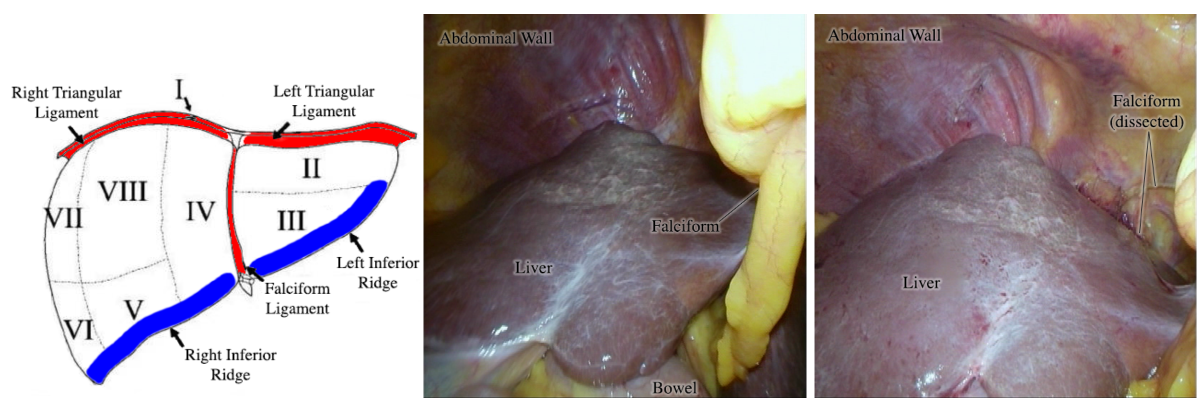

Figure 1. Left: Diagram of the anatomical positions of the falciform and triangular ligaments on the liver (red) and the left and right inferior ridges (blue), adapted from Kingham et al.[9] Center: Anterior surface of the right lobe of the liver during a laparoscopic procedure. After insufflation, the liver suspends from its ligaments and rests on the bowel. Note the tension where the liver attaches to the falciform ligament. Right: Anterior surface of the liver after dissection of the falciform and right triangular ligaments. The tension held by the ligaments relaxes and the shape of the liver changes, indicating intraoperative deformation. The phantom system aims to reproduce the distinct sources of deformation unique to laparoscopic procedures.

1.1 Objective

The purpose of this work is (1) to create a mock surgical system that reflects the dynamics of the intraoperative laparoscopic environment and (2) to demonstrate a system that can quantitatively assess registration accuracy in the setting of laparoscopic image-guided liver resection. Registration accuracy is assessed using the phantom and two laparoscopic methods of sparse intraoperative surface data collection. Rigid registration remains the standard registration method in clinically approved IGLS systems for open surgery, although no standard yet exists for laparoscopic IGLS. This preliminary study will establish a foundation for validating further developments in laparoscopic image guidance.

2. METHODS

A phantom system was designed to reproduce the intraoperative conditions of laparoscopic liver procedures. The setup consists of an abdominal frame that mimics the insufflated abdomen, inside of which a soft tissue liver phantom is suspended. We use this mock laparoscopic setup to perform a preliminary analysis of rigid registration accuracy in the laparoscopic setting with regard to data acquired through various ports and with two different methods of intraoperative data acquisition. A qualitative comparison is also performed between the deformation produced by the phantom and the deformation observed *in vivo* during laparoscopic liver resection.

2.1 Laparoscopic Phantom System

To match the dimensions of the insufflated abdominal wall reported by Song et al.[10], the abdominal frame was constructed from a half-pipe of an 18-inch diameter PVC sleeve. Nine ports were placed in the mock abdominal wall to mimic laparoscopic access ports to the abdominal cavity. The mock ports were placed in accordance with commonly used port positions for laparoscopic right and left lobe liver resection as reported by Cho et al.[11] and Cherqui et al.[12] The mock abdomen was mounted on four extensible legs to permit inclines between -30° and +30° as a patient may experience intraoperatively. Furthermore, the legs carry a platform that can be raised or lowered to apply or remove support from the bowel on the posterior of the liver. To provide locations for ligament attachment, supporting bars were attached to the interior of the abdominal cavity. A silicone liver phantom was suspended from these supporting bars at the falciform ligament, left triangular ligament, and right triangular ligament by Velcro® loop fabric strips. Any combination of the Velcro® attachments can be removed to simulate dissection of ligaments. Figure 2 shows the abdominal frame suspending the phantom before and after right lobe mobilization. Note that the primary structures providing mechanical support to the phantom are the ligament connections and a mock bowel placed beneath the liver, as is the case *in vivo* (Figure 1). Finally, a rigid body fiducial was attached to the exterior of the abdominal frame to provide a reference for the optical tracking system in the registration study.

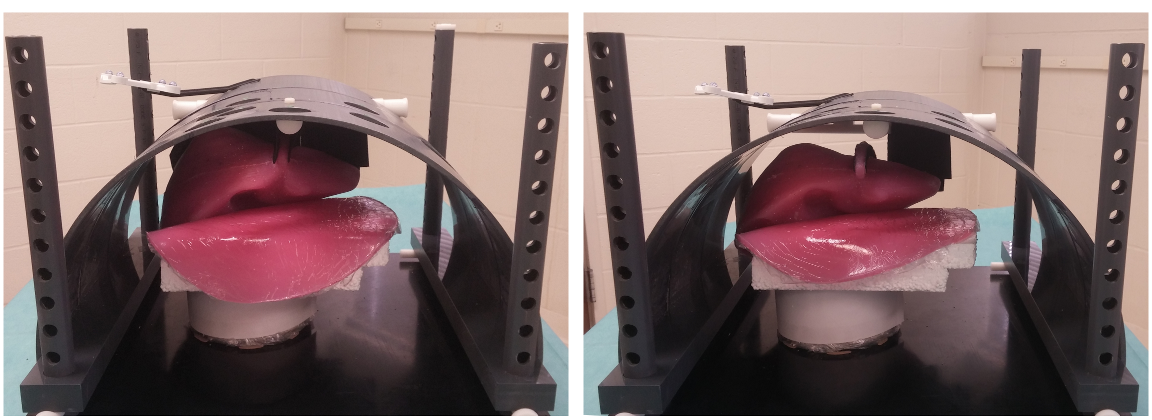

Figure 2. Inferior view of the soft-tissue liver phantom in the laparoscopic abdominal frame with (left) and without (right) support from the falciform and right triangular ligaments, simulating right lobe mobilization. Note the deformation that has occurred following removal of the ligament attachments to the liver.

A soft-tissue liver phantom was made from Ecoflex® 00-10 platinum-cure silicone (Smooth-On Inc., PA) mixed with Silicone Thinner® (31% mass) to decrease silicone stiffness and Slacker® Tactile Mutator (23% mass) to provide viscosity (Smooth-On Inc., PA). A mold for the liver phantom was created from a preoperative human CT scan. The mold was recast in plaster and modified to include 1.5 cm protrusions along the falciform, left triangular, and right triangular ligaments. After the phantom was removed from the mold, Velcro® hook strips were adhered to the protrusions using Sil-Poxy® Silicone Epoxy (Smooth-On Inc., PA) to complete the suspension mechanism from the abdominal frame. A total of 147 radiopaque plastic beads and 1-mm stainless steel ball bearings were embedded in the phantom to serve as targets in CT images for quantitative validation of registration accuracy. The distribution of targets is shown in Figure 3.

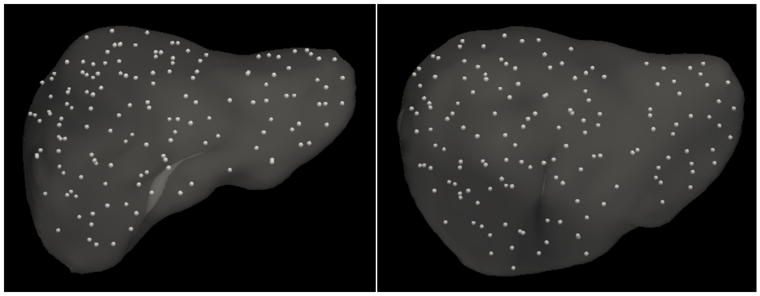

Figure 3. Target positions within the soft tissue phantom from the anterior view (left) and anterosuperior view (right). The 147 targets are dispersed consistently throughout the volume of the phantom.

2.2 Laparoscopic Registration Study

The described phantom system was used to perform and evaluate the accuracy of laparoscopic liver registrations. This process consisted of: (1) acquiring and processing preoperative and intraoperative CT scans of the phantom, (2) collecting intraoperative surface data, and (3) registering the intraoperative data and evaluating registration accuracy. To compare phantom and *in vivo* deformation, registrations using intraoperative surface data from the phantom were qualitatively compared to those using clinical intraoperative surface data from a previous study on laparoscopic IGLS.

2.2.1 CT Imaging and Segmentation

A preoperative CT of the liver phantom with embedded targets was acquired with the phantom inside a mold constructed from a clinical tomogram of a human liver. The phantom was removed from the mold and suspended in the abdominal frame, set at an incline of 16.7°. Left- and right-lobe mobilization were simulated by removing the falciform and the left or right triangular Velcro® ligaments, respectively. Intraoperative tomograms of the liver phantom and embedded targets were acquired with 0.62×0.62×3 mm voxel spacing for both conditions of mobilization. Manual segmentation was performed to remove the ligament protrusions added to the phantom and to correctly establish correspondence between targets in the preoperative and intraoperative scans.

2.2.2 Collection of Intraoperative Sparse Surface Data

Intraoperative data consisted of sparse point clouds of the anterior surface of the liver, collected for left and right mobilization conditions through each of the nine ports. Following the salient feature weighted iterative closest point (wICP) method in Clements et al.[3], sparse collections along three features (the falciform ligament, the left inferior ridge, and the right inferior ridge, see Figure 1) and the rest of the anterior surface were obtained. Two methods were used to acquire these sparse surfaces through the laparoscopic access ports. First, a trocar-compatible optically tracked stylus was used to manually swab the surface of the organ. Second, a trocar-compatible optically tracked handheld conoprobe MK3[13,14] (Optimet Inc., Jerusalem, Israel) was used to obtain similar data in a non-contact manner. Optical tracking was accomplished with an NDI Polaris Spectra camera (Northern Digital Inc., Waterloo, Canada). The experimental setup of the conoprobe and the port locations on the abdominal frame are shown in Figure 4.

2.2.3 Registration to Intraoperative Data

The salient feature wICP method described by Clements et al.[3] was used to rigidly register the intraoperative sparse surface data and the intraoperative target positions to the preoperative anatomy. It should be noted that some features could not be accessed through several ports due to limited range of motion or line of sight with the optical tracking system, leading to some registrations being performed with fewer than three features. To measure the accuracy of the registration, target registration error (TRE) was computed as the Euclidean distance between the preoperative and registered intraoperative targets. A registration to the entire segmented surface of the intraoperative CT was also performed to represent the ideal rigid alignment.

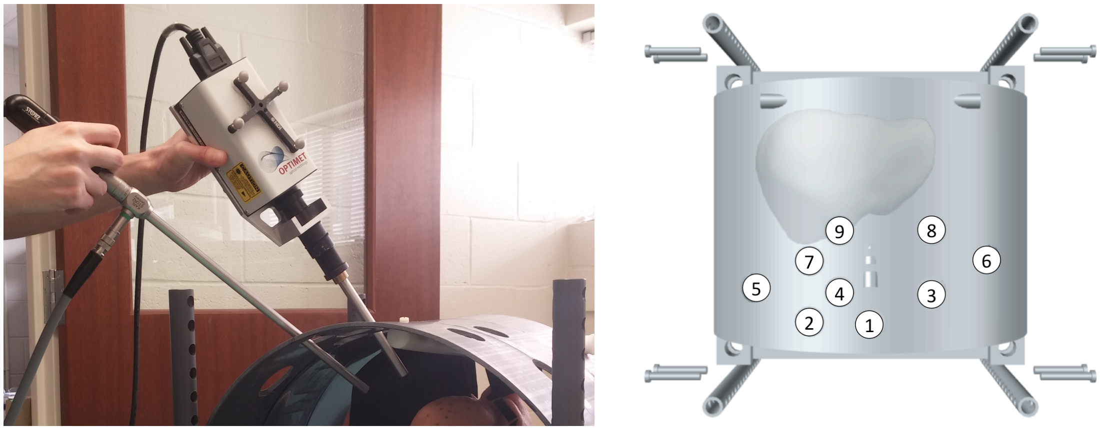

Figure 4. Left: Experimental setup of intraoperative data collection using the conoprobe. The conoprobe laser beam can be guided by a laparoscope. Right: Placement of the nine access ports in the abdominal frame. Port 1 is located at the umbilicus.

2.2.4 Comparison to Clinical Deformation

Clinical laparoscopic image guidance data were obtained from a previous study by Kingham et al.[9] at Memorial Sloan-Kettering Cancer Center. Following rigid registration, the non-rigid misalignment resulting from *in vivo* deformation and the phantom deformation were qualitatively compared to estimate the suitability of the phantom system for reproducing laparoscopic deformation.

3. RESULTS

A summary in Table 1 shows the registration outcomes for left and right mobilization conditions using stylus and conoprobe acquisition through the umbilicus port, compared with a registration with ideal data using the full intraoperative surface from CT. In both states of deformation, the registration using data from the conoprobe achieves lower average TRE and smaller standard deviations of target error than registrations to stylus-collected data. Additionally, the TRE for data acquired through each of the nine ports are shown in Figure 5. Data acquired through the periumbilical ports tended to produce the best registrations, and lateral and superior ports could not access some salient features. These tendencies suggest that the region of data accessible through various ports is important to the process of registration. Across all ports, registrations using the conoprobe improved the average TRE by 2.0 mm, although the difference was not statistically significant (p=0.18, paired sample t-test, N=18).

Table 1. Target registration error (mean ± SD) for simulated right and left lobe mobilization using stylus and conoprobe sparse surface acquisitions through the umbilicus port and the ideal registration using the intraoperative organ configuration from CT.

Acquisition Method	Left Mobilization	Right Mobilization
Stylus	14.8 ± 5.6 mm	16.9 ± 7.0 mm
Conoprobe	13.0 ± 2.6 mm	11.4 ± 5.5 mm
Intraoperative CT	12.4 ± 2.5 mm	12.3 ± 4.8 mm

A comparison between rigid registrations (Figure 6) using clinical data from a previous laparoscopic image guidance study and phantom data from our laparoscopic system shows similar shift between the shape of the preoperative liver and the intraoperative surface. The similarity indicates that the phantom system is capable of producing organ deformation in agreement with the deformation seen *in vivo*.

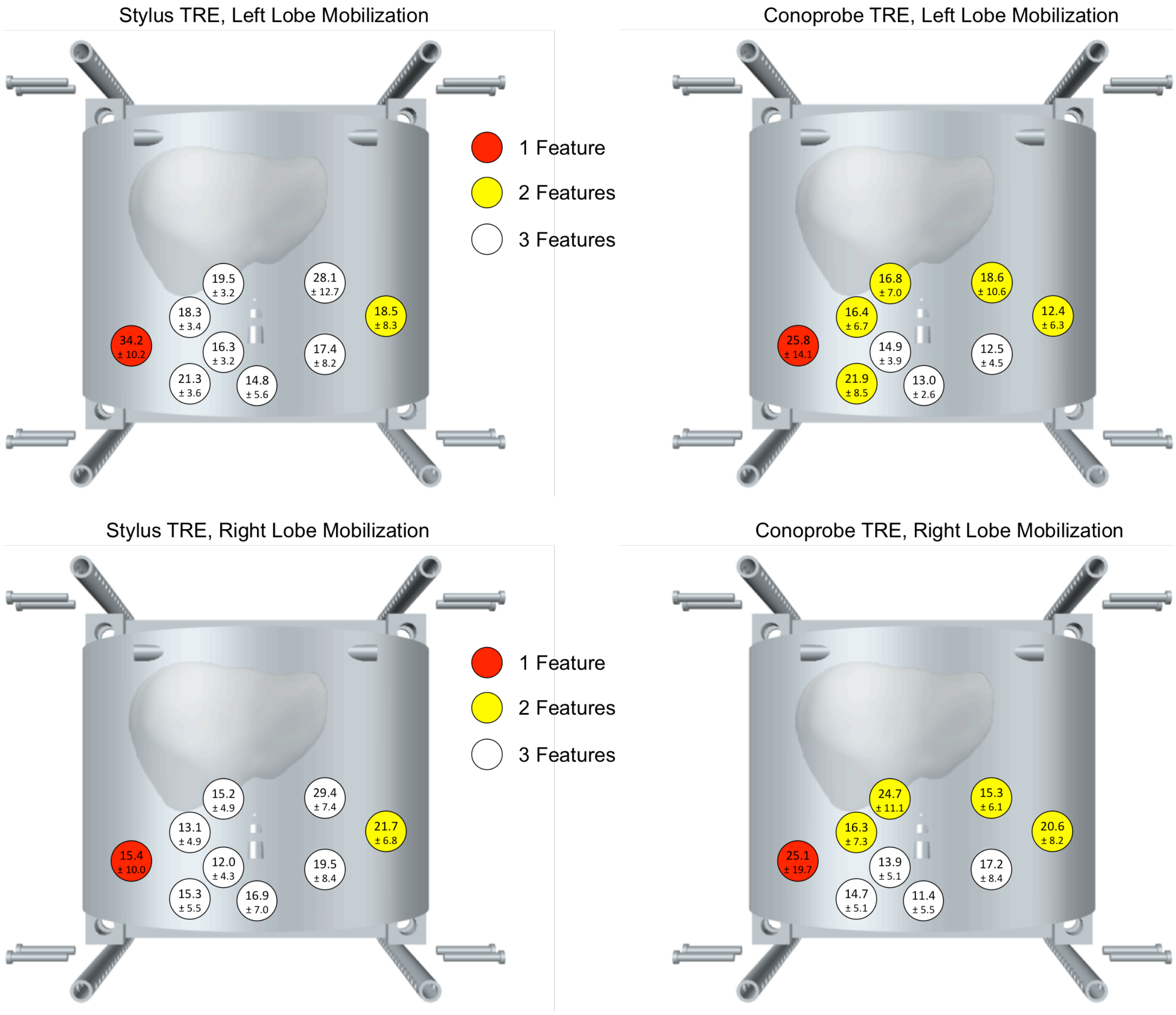

Figure 5. Target registration error in mm (mean ± SD) for simulated left lobe (top row) and right lobe (bottom row) mobilization using stylus (left column) and conoprobe (right column) acquisition from each port. Ports near the umbilicus have the best access to the features used in the wICP rigid registration method. Ports colored red, yellow, and white could access only one, two, or all three of the features, respectively. The extent of data accessible through the lateral and superior ports tended to limit feature acquisition with the conoprobe.

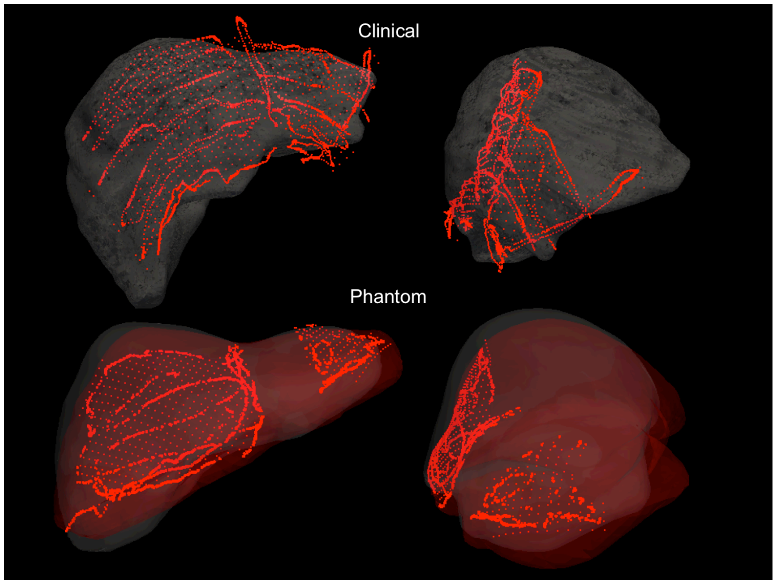

Figure 6. Anterior view (left) and lateral view (right) of the observed deformation in a clinical laparoscopic case (top) compared to a phantom case (bottom). The white surface indicates the shape of the segmented preoperative liver and the red points indicate the rigidly registered intraoperative sparse surface data. To ease visual comparison, a spatial interpolation method was applied to produce an evenly spaced sampling of the best-fit intraoperative surface described by the sparse data collection. The red surface in the phantom case is the registered intraoperative configuration segmented from CT. In both scenarios, the registered intraoperative surface on the right lobe resides beneath the preoperative surface. The intraoperative CT of the phantom suggests the apparent flattening of the right lobe could result from shifting tension on the ligaments after insufflation distends the abdominal wall and diaphragm.

4. DISCUSSION

On average, sparse intraoperative surface data collected with the conoprobe resulted in rigid registrations with mean TRE of 2.0 mm less than those of registrations using surface data collected with the laparoscopic stylus. The tracked conoprobe may yield better registration outcomes due to its non-contact nature, whereas the tracked stylus may be prone to error due to the need for direct contact with the organ surface and difficulty coordinating the tip of the stylus in laparoscopic applications, where a fulcrum at the port mirrors motion and a long lever arm accentuates it. While the reduction in TRE between stylus and conoprobe acquisitions was not found to be statistically significant, there are a number of confounding factors that impair direct comparison. First, the extents of data accessible with the conoprobe and stylus differ. While the conoprobe is capable of accurate measurement at angles of incidence up to 85º, in practice the tracked conoprobe has smaller coverage on the organ surface. The smaller surface coverage stems from difficulty measuring along the boundary of the liver due to handheld tremble potentially causing the conoprobe laser beam to leave the liver surface. Second, the absence of accessible salient features from several of the ports may impair the robustness of the registration algorithm. However, it is interesting to note that among ports which have all three features available in both the conoprobe and stylus acquisitions, the mean TRE of registrations using conoprobe surface data are still on average 2.1 mm smaller than the TRE of corresponding registrations with stylus surface data (p=0.07, paired sample t-test, N=7). Despite the lack of demonstrated statistical significance, the sample sizes in this preliminary study are too small to provide adequate statistical power. While registration accuracies between the two intraoperative surface acquisition methods remain comparable, further data from additional phantoms under varying states of mobilization are required to better understand the tradeoffs between the conoprobe and stylus.

The smallest magnitude of mean TRE we observed among all registrations was 11.4±5.5 mm. Rigid registrations using complete organ surface data from the intraoperative CT produced TRE exceeding 12 mm in both left and right mobilization conditions. From these large magnitudes, we note that substantial non-rigid deformation may exist. This assertion is corroborated by the deformation observed in Figure 6, where the shapes of the preoperative and the registered intraoperative livers evidently differ. These findings suggest that rigid registration alone is not completely suitable for laparoscopic registration. Future work will include development of non-rigid registration algorithms for the liver in the laparoscopic environment to better account for this deformation.

5. CONCLUSIONS

In this work, we have developed a laparoscopic liver phantom system that reproduces the intraoperative sources of deformation existing in laparoscopic procedures. Furthermore, we demonstrate that this phantom system can be used to quantitatively assess registration accuracy through computation of target registration error between preoperative and intraoperative post-deformation CT scans of the phantom. This contribution is valuable because it permits direct and quantitative validation of laparoscopic IGLS registration methodologies without introducing significant clinical burden. Our preliminary work indicates that this mock system produces deformation similar to that observed during *in vivo* procedures. An initial study of rigid registration accuracy suggests that registration accuracy may depend on the port through which data is collected, and hence the region of the organ accessed. Moreover, the presence of substantial soft tissue deformation may require development of non-rigid registration methodologies for laparoscopic IGLS.

ACKNOWLEDGEMENTS

This work was supported by the NIH grant R01-CA162477 and the NIH-NIBIB training grant T32-EB021937. We would like to thank the Vanderbilt Machine Shop for assistance in constructing the abdominal frame of the phantom.

REFERENCES

[1] Heizmann, O., Zidowitz, S., Bourquain, H., Potthast, S., Peitgen, H. O., Oertli, D.., Kettelhack, C., "Assessment of intraoperative liver deformation during hepatic resection: Prospective clinical study," World J. Surg. **34**(8), 1887–1893 (2010).

[2] Clements, L. W., Collins, J. A., Simpson, A. L., Adams, L. B., Jarnagin, W. R.., Miga, M. I., "Evaluation of model-based deformation correction in image-guided liver surgery via tracked intraoperative ultrasound," Med. Imaging **3**(1), 1–10 (2016).

[3] Clements, L. W., Chapman, W. C., Dawant, B. M., Galloway, R. L.., Miga, M. I., "Robust surface registration using salient anatomical features for image-guided liver surgery: algorithm and validation.," Med. Phys. **35**(6), 2528–2540 (2008).

[4] Rucker, D., Wu, Y., Clements, L., Ondrake, J., Pheiffer, T., Simpson, A., Jarnagin, W.., Miga, M., "A Mechanics-Based Nonrigid Registration Method for Liver Surgery using Sparse Intraoperative Data.," IEEE Trans. Med. Imaging **33**(1), 147–158 (2014).

[5] Thompson, S., Totz, J., Song, Y., Johnsen, S., Stoyanov, D., Ourselin, S., Gurusamy, K., Scheider, C., Davidson, B., et al., "Accuracy validation of an image guided laparoscopy system for liver resection," Proc. SPIE **9415**, 1–12 (2015).

[6] Banovac, F., Tang, J., Xu, S., Lindisch, D., Chung, H. Y., Levy, E. B., Chang, T., McCullough, M. F., Yaniv, Z., et al., "Precision targeting of liver lesions using a novel electromagnetic navigation device in physiologic phantom and swine.," Med. Phys. **32**(8), 2698–2705 (2005).

[7] Wu, Y., Rucker, D. C., Conley, R. H., Pheiffer, T. S., Simpson, A. L., Geevarghese, S. K.., Miga, M. I., "Registration of liver images to minimally invasive intraoperative surface and subsurface data," Proc. SPIE Med. Imaging **9036**, 1–8 (2014).

[8] Zijlmans, M., Langø, T., Hofstad, E. F., Van Swol, Christiaan, F. P.., Rethy, A., "Navigated laparoscopy – liver shift and deformation due to pneumoperitoneum in an animal model," Minim. Invasive Ther. **21**, 241–248 (2012).

[9] Kingham, T. P., Jayaraman, S., Clements, L. W., Scherer, M. A., Stefansic, J. D.., Jarnagin, W. R., "Evolution of Image-Guided Liver Surgery: Transition from Open to Laparoscopic Procedures," J Gastrointest Surg **17**, 1274–1282 (2013).

[10] Song, C., Alijani, A., Frank, T., Hanna, G. B.., Cuschieri, A., "Mechanical properties of the human abdominal wall measured in vivo during insufflation for laparoscopic surgery," Surg. Endosc. **20**(6), 987–990 (2006).

[11] Cho, J. Y., Han, H.-S., Yoon, Y.-S.., Shin, S.-H., "Outcomes of Laparoscopic Liver Resection for Lesions Located in the Right Side of the Liver," Arch Surg **144**(1), 25–29 (2009).

[12] Cherqui, D., Husson, E., Hammoud, R.., Malassagne, B., "Laparoscopic Liver Resections : A Feasibility Study in 30 Patients," Ann. Surg. **232**(6), 753–762 (2000).

[13] Burgner, J., Simpson, A. L., Fitzpatrick, J. M., Lathrop, R. A., Herrell, S. D., Miga, M. I.., Webster, R. J., "A study on the theoretical and practical accuracy of conoscopic holography-based surface measurements: Toward image registration in minimally invasive surgery," Int. J. Med. Robot. Comput. Assist. Surg. **9**(2), 190–203 (2013).

[14] Lathrop, R. A., Hackworth, D. M.., Webster, R. J., "Minimally Invasive Holographic Surface Scanning for Soft-Tissue Image Registration," IEEE Trans. Biomed. Eng. **57**(6), 1497–1506 (2014).